Journal of Nuclear Materials 403 (2010) 1–6

Contents lists available at ScienceDirect

Journal of Nuclear Materials

journal homepage: www.elsevier.com/locate/jnucmat

Thermodynamic modeling of the Pb–U and Pb–Pu systems

Z.S. Li, X.J. Liu, C.P. Wang *

Department of Materials Science and Engineering, College of Materials, and Research Center of Materials Design and Applications, Xiamen University, Xiamen 361005, PR China

ARTICLE INFO

Article history:
Received 21 October 2009
Accepted 3 February 2010

ABSTRACT

The thermodynamic assessments of the Pb–U and Pb–Pu binary systems were carried out using the CALPHAD (calculation of phase diagrams) method based on experimental data for thermodynamic properties and phase equilibria. The Gibbs free energies of the liquid, bcc, fcc, (αU), (βU), (δ′Pu), (γPu), (βPu) and (αPu) phases were described by a subregular solution model with the Redlich–Kister equation, and those of the intermetallic compounds (Pb_3U, PbU, $PbPu_3$, Pb_3Pu_5, Pb_4Pu_5, Pb_5Pu_4, αPb_2Pu, βPb_2Pu and Pb_3Pu) by a two-sublattice model. The thermodynamic parameters for the two binary systems were optimized to consistently reproduce the available experimental data with satisfactory agreement.

1. Introduction

A good understanding of nuclear materials is important to develop a safe nuclear reactor with high efficiency [1,2], and the investigation of phase diagrams is essential for the development of new nuclear materials. Our goal is to develop a database of thermodynamic data and phase diagrams for nuclear materials. However, traditional methods of materials research solely based on experimental investigations are far from being suitable for probing nuclear materials properties because of the stringent experimental conditions. A better approach is to investigate first the relevant phase diagrams of nuclear materials that are crucial for the development of advanced nuclear fuels. The present authors, therefore, have been conducting thermodynamic assessments in nuclear material systems using CALPHAD (calculation of phase diagrams) technique [3–9]. As a part of this thermodynamic database, the present work focuses on thermodynamic assessment of the Pb–U and Pb–Pu phase diagrams based on the CALPHAD method from available experimental data. Uranium (U) and plutonium (Pu) are the most common fissile elements in the nuclear fuel, and lead (Pb) is a primary coolant and spallation target material for the next generation of accelerator-driven systems (ADS) [10–12]. Thus, it is important to evaluate the interaction between metal fuel and lead coolant. In this work the phase diagram and the thermodynamic data for the Pb–U and Pb–Pu systems are assessed.

2. Thermodynamic model

2.1. Modeling procedure

Optimization of the thermodynamic parameters describing the Gibbs free energies of each phase is carried out using the PARROT module of the Thermo-Calc software [13], a computer program that can accept different types of data, such as thermodynamic quantities and phase equilibria. Each selected data is given a certain weight and the weight can be changed until a satisfactory description for most of the selected data is achieved. The information on stable phases and the used models for the Pb–U and Pb–Pu systems is listed in Table 1.

2.2. Solution phases

The Gibbs free energies of the solution phases of the Pb–Me (Me:Pu, U) systems were described by a subregular solution model [14]. The molar Gibbs free energy of each solution phase in the Pb–Me system was given as follows:

$$G_m^{\phi} = \sum_{i=\mathrm{Pb,Me}} {}^{0}G_i^{\phi} x_i + \mathrm{RT} \sum_{i=\mathrm{Pb,Me}} x_i \ln x_i + {}^{E}G_m^{\phi}, \quad (1)$$

where ${}^{0}G_i^{\phi}$ is the molar Gibbs free energy of pure component i with respect to their respective reference state ϕ phase, which was taken from the SSOL4 database [15]. R is the gas constant, T is the absolute temperature in Kelvin, and x_i denotes the mole fraction of component i. The term ${}^{E}G_m^{\phi}$ is the excess energy, which was expressed by a Redlich–Kister polynomials [16] as:

* Corresponding author. Tel.: +86 592 2180606; fax: +86 592 2187966.
E-mail address: wangcp@xmu.edu.cn (C.P. Wang).

0022-3115/$ - see front matter © 2010 Elsevier B.V. All rights reserved.
doi:10.1016/j.jnucmat.2010.02.002

Table 1
The stable phases and the models used for the Pb–U and Pb–Pu systems.

System	Phase	Prototype	Strucktur-bericht designation	Modeling phase	Used models
Pb–U	(Pb)	Cu	A1	(Pb, U)	Subregular solution model
	Pb_3U	$AuCu_3$	$L1_2$	$(Pb)_3(U)_1$	Two-sublattice model
	PbU	PbU	–	$(Pb)_1(U)_1$	Two-sublattice model
	γU	W	A2	(Pb, U)	Subregular solution model
	βU	βU	A_b	(Pb, U)	Subregular solution model
	αU	αU	A20	(Pb, U)	Subregular solution model
	Liquid	–	–	(Pb, U)	Subregular solution model
Pb–Pu	(Pb)	Cu	A1	(Pb, Pu)	Subregular solution model
	$PbPu_3$	$AuCu_3$	$L1_2$	$(Pb)_1(Pu)_3$	Two-sublattice model
	Pb_3Pu_5	Si_3W_5	$D8_m$	$(Pb)_3(Pu)_5$	Two-sublattice model
	Pb_4Pu_5	Ga_4Ti_5	–	$(Pb)_4(Pu)_5$	Two-sublattice model
	Pb_5Pu_4	–	–	$(Pb, Pu)_5(Pb, Pu)_4$	Two-sublattice model
	βPb_2Pu	–	–	$(Pb)_2(Pu)_1$	Two-sublattice model
	αPb_2Pu	Ga_2Hf	–	$(Pb)_2(Pu)_1$	Two-sublattice model
	Pb_3Pu	$AuCu_3$	$L1_2$	$(Pb)_3(Pu)_1$	Two-sublattice model
	εPu	W	A2	(Pb, Pu)	Subregular solution model
	δ′Pu	In	A6	(Pb, Pu)	Subregular solution model
	δPu	Cu	A1	(Pb, Pu)	Subregular solution model
	γPu	–	–	(Pb, Pu)	Subregular solution model
	βPu	–	–	(Pb, Pu)	Subregular solution model
	αPu	–	–	(Pb, Pu)	Subregular solution model
	Liquid	–	–	(Pb, Pu)	Subregular solution model

$$ {}^{E}G_m^{\phi} = x_{\mathrm{Pb}} x_{\mathrm{Me}} \sum_{m=0}^{n} {}^{m}L_{\mathrm{Pb,Me}}^{\phi} (x_{\mathrm{Pb}} - x_{\mathrm{Me}})^m, \tag{2} $$

The x_{Pb} and x_{Me} are the mole fractions of Pb and Me components, and ${}^{m}L_{\mathrm{Pb,Me}}^{\phi}$ is the interaction energy between Pb and Me atoms, and was expressed as:

$$ {}^{m}L_{\mathrm{Pb,Me}}^{\phi} = a_m + b_m T. \tag{3} $$

The parameters a_m and b_m were evaluated from experimental data in the present work.

2.3. Stoichiometric intermetallic compounds

The Pb_3U, PbU, $PbPu_3$, Pb_3Pu_5, Pb_4Pu_5, αPb_2Pu, βPb_2Pu and Pb_3Pu compounds were treated as stoichiometric phases. The Gibbs free energy of formation per mole of formula unit $(Pb)_m(Me)_n$ can be expressed by a two-sublattice model [17] by the following equation with reference to the pure elements in their non-magnetic state:

$$ \Delta G_f^{\mathrm{Pb}_m\mathrm{Me}_n} = {}^{0}G_{\mathrm{Pb:Me}}^{\mathrm{Pb}_m\mathrm{Me}_n} - m\,{}^{0}G_{\mathrm{Pb}}^{\mathrm{ref}} - n\,{}^{0}G_{\mathrm{Me}}^{\mathrm{ref}} = a' + b'T, \tag{4} $$

where $\Delta G_f^{\mathrm{Pb}_m\mathrm{Me}_n}$ denotes the standard Gibbs free energy of formation of the stoichiometric compound with reference to the pure elements. The terms ${}^{0}G_{\mathrm{Pb}}^{\mathrm{ref}}$ and ${}^{0}G_{\mathrm{Me}}^{\mathrm{ref}}$ are the molar Gibbs free energy of pure element Pb and Me with its defined reference structure in a non-magnetic state. The parameters a' and b' were evaluated in the present optimization.

2.4. Non-stoichiometric intermetallic phases

The Pb_5Pu_4 phase in the Pb–Pu binary system was treated as a non-stoichiometric intermetallic phase, because there was a significant composition range in the Pb_5Pu_4 phase at higher temperatures [18]. The Gibbs free energy of the Pb_5Pu_4 phase was also described by a two-sublattice model [17]. The Gibbs free energy of formation per mole of formula unit $(Pb, Pu)_5(Pb, Pu)_4$ can be expressed as the following equation with reference to the pure elements in their non-magnetic state:

$$ \begin{aligned} G_m^{\mathrm{Pb_5Pu_4}} = {} & y_{\mathrm{Pb}}^{\mathrm{I}} y_{\mathrm{Pb}}^{\mathrm{II}}\, {}^{0}G_{\mathrm{Pb:Pb}} + y_{\mathrm{Pb}}^{\mathrm{I}} y_{\mathrm{Pu}}^{\mathrm{II}}\, {}^{0}G_{\mathrm{Pb:Pu}} + y_{\mathrm{Pu}}^{\mathrm{I}} y_{\mathrm{Pb}}^{\mathrm{II}}\, {}^{0}G_{\mathrm{Pu:Pb}} + y_{\mathrm{Pu}}^{\mathrm{I}} y_{\mathrm{Pu}}^{\mathrm{II}}\, {}^{0}G_{\mathrm{Pu:Pu}} \\ & + 5\mathrm{RT}\left(y_{\mathrm{Pb}}^{\mathrm{I}} \ln y_{\mathrm{Pb}}^{\mathrm{I}} + y_{\mathrm{Pu}}^{\mathrm{I}} \ln y_{\mathrm{Pu}}^{\mathrm{I}}\right) + 4\mathrm{RT}\left(y_{\mathrm{Pb}}^{\mathrm{II}} \ln y_{\mathrm{Pb}}^{\mathrm{II}} + y_{\mathrm{Pu}}^{\mathrm{II}} \ln y_{\mathrm{Pu}}^{\mathrm{II}}\right) \\ & + 5 y_{\mathrm{Pb}}^{\mathrm{I}} y_{\mathrm{Pu}}^{\mathrm{I}} \left[y_{\mathrm{Pb}}^{\mathrm{II}} \sum_n {}^{n}L_{\mathrm{Pb,\,Pu:Pb}} \left(y_{\mathrm{Pb}}^{\mathrm{I}} - y_{\mathrm{Pu}}^{\mathrm{I}}\right)^n + y_{\mathrm{Pu}}^{\mathrm{II}} \sum_n {}^{n}L_{\mathrm{Pb,\,Pu:Pu}} \left(y_{\mathrm{Pb}}^{\mathrm{I}} - y_{\mathrm{Pu}}^{\mathrm{I}}\right)^n \right] \\ & + 4 y_{\mathrm{Pb}}^{\mathrm{II}} y_{\mathrm{Pu}}^{\mathrm{II}} \left[y_{\mathrm{Pb}}^{\mathrm{I}} \sum_n {}^{n}L_{\mathrm{Pb:Pb,\,Pu}} \left(y_{\mathrm{Pb}}^{\mathrm{II}} - y_{\mathrm{Pu}}^{\mathrm{II}}\right)^n + y_{\mathrm{Pu}}^{\mathrm{I}} \sum_n {}^{n}L_{\mathrm{Pu:Pb,\,Pu}} \left(y_{\mathrm{Pb}}^{\mathrm{II}} - y_{\mathrm{Pu}}^{\mathrm{II}}\right)^n \right], \end{aligned} \tag{5} $$

where y_i^{I} and y_j^{II} are the site fractions of component i and j (i, j = Pb, Pu) located on sublattice I and II, respectively, and the parameters ${}^{0}G_{i:j}$ represents the Gibbs free energy of the compound phase when the two sublattices are occupied by element i or j. $L_{i:\mathrm{Pb,Pu}}$ and $L_{\mathrm{Pb,Pu}:j}$ are the interaction parameter between Pb and Pu in the second or first sublattice, when the other sublattice is occupied by element i or j. ${}^{0}G_{i:j}$, $L_{i:\mathrm{Pb,Pu}}$ and $L_{\mathrm{Pb,Pu}:j}$ were evaluated in the present work.

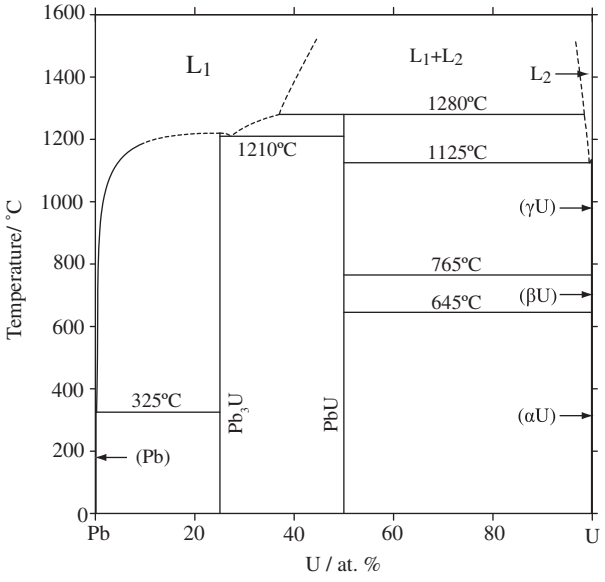

Fig. 1. The Pb–U phase diagram reviewed by Sheldon et al. [23].

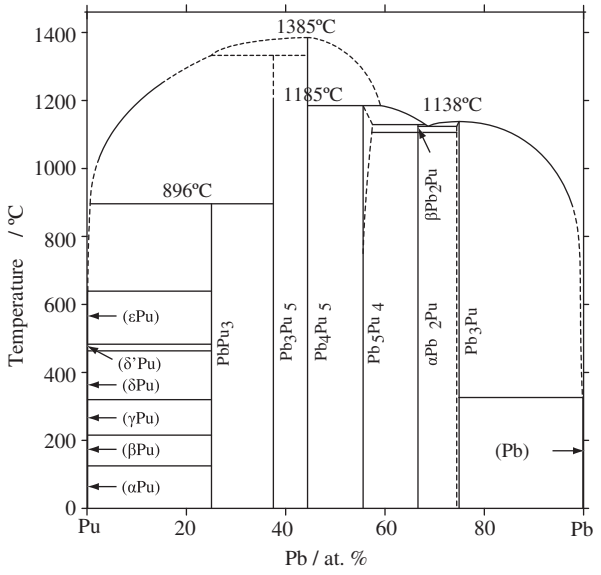

Fig. 2. The Pb–Pu phase diagram reviewed by Foltyn et al. [29].

3. Experimental information

3.1. The Pb–U system

The phase diagram of the Pb–U system has been investigated by many researchers [18–23]. The first comprehensive investigation of the phase diagram in the Pb–U system was published by Teitel [19]. Teitel's investigation [19] of the Pb_3U phase gives a melting point in the1210–1250 °C temperature range with a recommended value of 1220 °C. Teitel [19] also found that there is a liquid miscibility gap above 1280 °C and little solubility of U in the Pb phase or Pb in the U-rich phases ((αU), (βU), (γU)) by X-ray diffraction, metallographic observation and thermal analysis. However, the accurate solubility range of the liquid miscibility gap was not determined due to experimental difficulties.

Much later, the Pb–U phase diagram was reviewed by Sheldon et al. [23] as shown in Fig. 1. The reviewed phase diagram consists of five solution phases (liquid, (Pb), (αU), (βU), (γU)) and two intermetallic compounds (Pb_3U and PbU). It also includes three eutectic reactions (L ↔ (Pb) + Pb_3U, L ↔ Pb_3U + PbU and L ↔ Pb–U + (γU)), a disputed syntectic reaction (L1 + L2 ↔ PbU) and a phase separation in the liquid phase at higher temperatures.

In addition, the enthalpies and entropies of formation of the compounds (Pb_3U and PbU) in the temperature range from 375 °C to 954 °C have been determined using vapour pressure measurement and EMF method respectively by many researchers [24–26]. Based on the above results, Chiotti et al. [27] calculated the enthalpies and entropies of formation of the compounds Pb_3U and PbU phases.

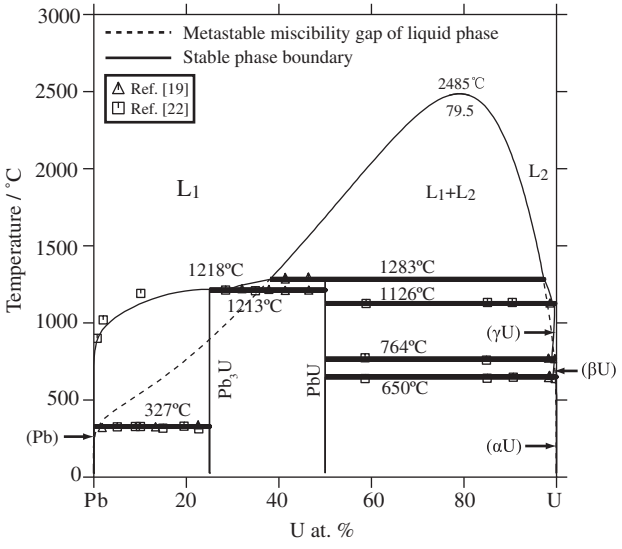

Fig. 3. Calculated Pb–U phase diagram with experimental data [19,22].

3.2. The Pb–Pu system

The most recent studies on the Pb–Pu system were reported by Wood et al. [18] and Nickerson [28] using differential thermal

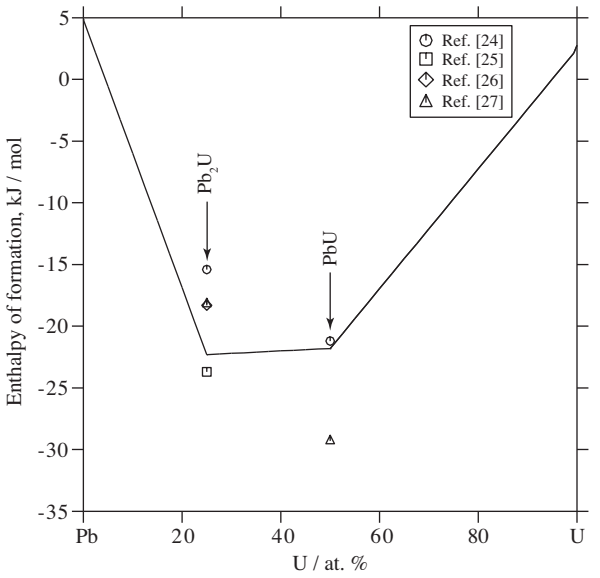

Fig. 4. Calculated enthalpies of formation of the intermetallic compounds at 677 °C in the Pb–U system compared with the experimental data [24–27]: the reference states are (αU) and fcc Pb phases.

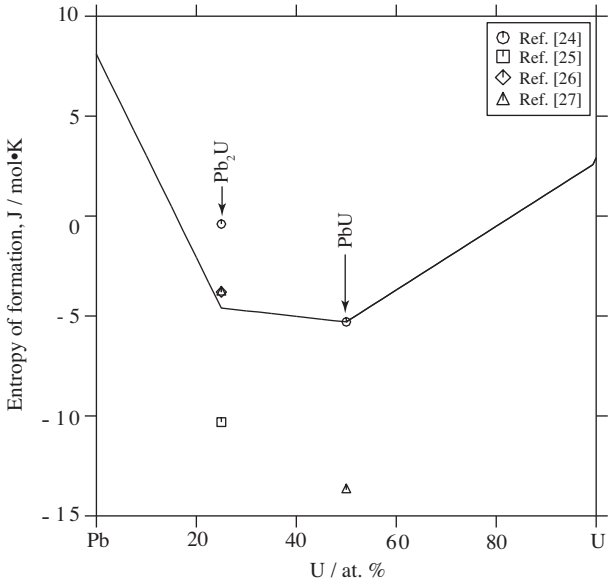

Fig. 5. Calculated entropies of formation of the intermetallic compounds at 677 °C in the Pb–U system compared with the experimental data [24–27]: the reference states are (αU) and fcc Pb phases.

Table 2
Parameters for each phase of the Pb–U system optimized in this work.

Parameters in each phase (J/mol) with temperature T in Kelvin
Liquid phase, format $(Pb, U)_1$
${}^0L^{Liq}_{Pb,U} = 81,158.96 - 47.628T$
${}^1L^{Liq}_{Pb,U} = -21,756.49 - 16.5T$
${}^2L^{Liq}_{Pb,U} = -20,700.2 + 9.61T$
${}^3L^{Liq}_{Pb,U} = 17,000$
A2 γU phase, format $(Pb, U)_1(Va)_3$
${}^0L^{bcc}_{Pb,U} = -24,950 + 45T$
${}^1L^{bcc}_{Pb,U} = 62,133 - 44T$
A_b βU phase, format $(Pb, U)_1$
${}^0G^{\beta U}_{Pb} = {}^0G^{fcc}_{Pb} + 5000$
${}^0L^{\beta U}_{Pb,U} = -26,820 + 50T$
${}^1L^{\beta U}_{Pb,U} = 67,820 - 50T$
A20 αU phase, format $(Pb, U)_1$
${}^0G^{\alpha U}_{Pb} = {}^0G^{fcc}_{Pb} + 20,000$
${}^0L^{\alpha U}_{Pb,U} = 0$
A1 (Pb) phase, format $(Pb, U)_1(Va)_1$
${}^0L^{fcc}_{Pb,U} = 0$
Pb_3U phase, format $(Pb)_{0.75}(U)_{0.25}$
${}^0G^{Pb_3U}_{Pb:U} = -22,300 + 4.6T + 0.75{}^0G^{fcc}_{Pb} + 0.25{}^0G^{\alpha U}_{U}$
Pb–U phase, format $(Pb)_{0.5}(U)_{0.5}$
${}^0G^{PbU}_{Pb:U} = -21,800 + 5.3T + 0.5{}^0G^{\alpha Pb}_{Pb} + 0.5{}^0G^{\alpha U}_{U}$

analysis, metallography, X-ray diffraction and electron microprobe analysis. Wood et al. [18] reported that six intermetallic compounds exist: $PbPu_3$, Pb_3Pu_5, Pb_4Pu_5, Pb_5Pu_4, Pb_2Pu and Pb_3Pu. According to their results, there is little solubility of Pb in the Pu-rich phases ((αPu), (βPu), (γPu), (δPu), (δ′Pu), (εPu)) and that of Pu in the Pb phase [18]. They also found that the Pb_3Pu_5 compound formed above 1300 °C by a peritectic reaction, $L + Pb_4Pu_5 \leftrightarrow Pb_3Pu_5$, although the accurate reaction temperature was not determined. The Pb_4Pu_5 phase has the highest melting point in the Pb–Pu system, located at approximate 1385 °C, also according to the work of Wood et al. [18]. Metallography results suggested a slight solubility of Pb in the Pb_5Pu_4 phase at higher temperature. The Pb_2Pu compound has a solid-state transformation at 1106 °C and is formed at 1129 °C by a peritectic reaction, $L + Pb_5Pu_4 \leftrightarrow Pb_2Pu$. Based on these works, Foltyn et al. reviewed the Pb–Pu phase diagram [29] as shown in Fig. 2.

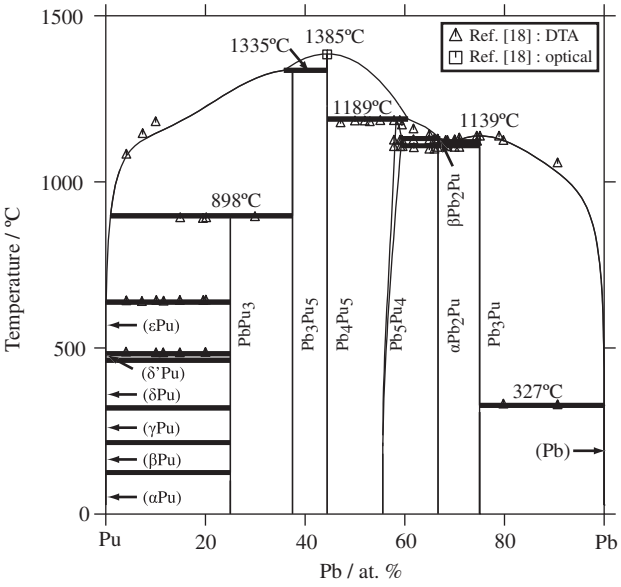

Fig. 6. Calculated Pb–Pu phase diagram with experimental data [18].

No experimental thermodynamic data for the compounds in the Pb–Pu system is available, but Chiotti [27] calculated the Gibbs energy of formation of the Pb_3Pu phase between 650 °C and 775 °C based on the data of Cafasso et al. [30].

4. Optimized results and discussion

4.1. The Pb–U system

The calculated Pb–U phase diagram with the experimental data [19,22] is shown in Fig. 3. This figure also shows the metastable liquid miscibility gap at lower temperatures with dashed lines. The calculated phase diagram was in agreement with the experimental data [19,22]. The calculated stable liquid miscibility gap region was between 38 and 97.2 at.% U, which agrees well with the experimental data [19]. The calculated critical composition and temperature of the liquid miscibility gap were 79.5 U at.% and 2485 °C, respectively. The calculated melting point of the Pb_3U phase was 1218 °C, which agrees with the result of Teitel [19]. In the U-rich region, little solubility of Pb in the (βU) and

Table 3
A comparison between the calculated invariant reactions and special points in the Pb–U system and the experimental results.

Reaction type	Reaction	U (at.%)			T (°C)	Reference
Eutectic	$L \leftrightarrow (Pb) + Pb_3U$	~0	0	25	325	[23]
		0	0	25	327	This work
Congruent	$L \leftrightarrow Pb_3U$		25		1220	[23]
			25		1218	This work
Eutectic	$L \leftrightarrow Pb_3U + PbU$	27.2	25	50	1210	[23]
		28.6	25	50	1213	This work
Syntectic	$L1 + L2 \leftrightarrow PbU$	37	98.5	50	1280	[23]
		38	97.2	50	1283	This work
Eutectic	$L \leftrightarrow Pb–U + \gamma U$	99.5	50	100	1125	[23]
		99.1	50	99.6	1126	This work
Eutectoid	$\gamma U \leftrightarrow \beta U + PbU$	~100	~100	50	765	[23]
		99.0	99.5	50	764	This work
Eutectoid	$\beta U \leftrightarrow \alpha U + PbU$	~100	~100	50	645	[23]
		99.2	99.9	50	650	This work
Critical	$L \leftrightarrow L1 + L2$		–		–	[23]
			79.5		2485	This work

(γU) phases is considered in the calculation. The calculated enthalpies and entropies of formation of the compounds at 677 °C are shown in Figs. 4 and 5, respectively, with the experimental data [24–27]. The experimental thermodynamic data obtained by different researchers differ somewhat from each other, and the calculated results of the present work are within the range of these values. The calculated enthalpies and entropies of formation of the PbU phase are in agreement with the experimental data of Alcock et al. [24], but slightly different from the calculated values of Chiotti et al. [27].

The complete set of the thermodynamic parameters describing the Gibbs free energy of each phase in the Pb–U system is given in Table 2, and all invariant reactions in the Pb–U system are summarized in Table 3, where the experimental data [23] are also listed for comparison.

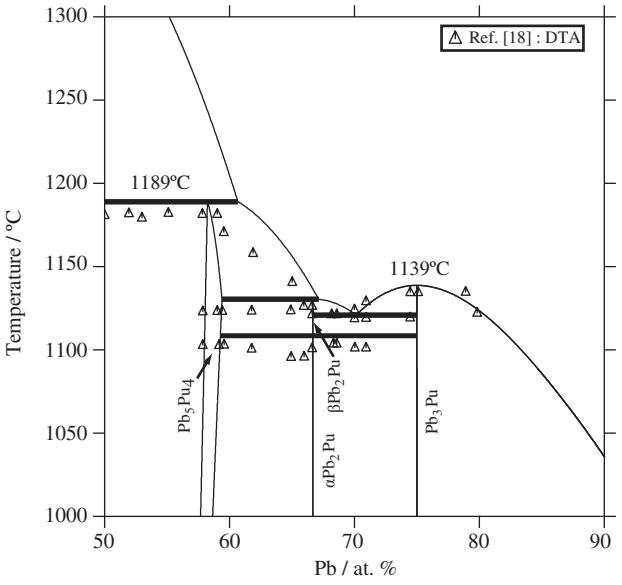

Fig. 7. Pb-rich portion of the calculated Pb–Pu phase diagram with experimental data [18].

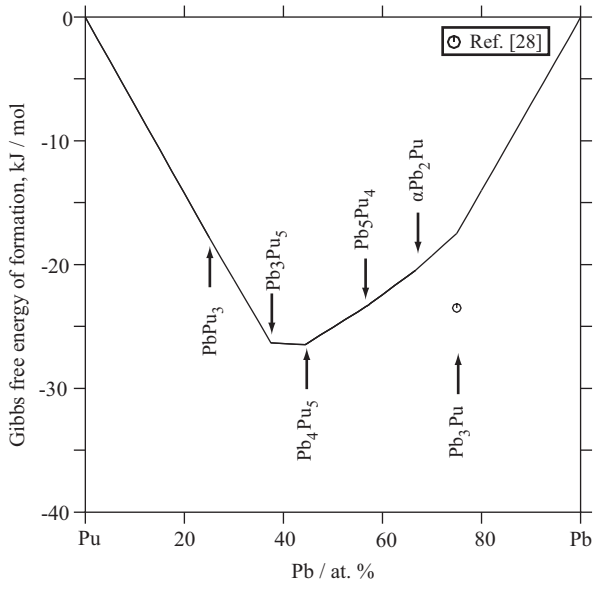

Fig. 8. Calculated Gibbs free energy at 727 °C in the Pb–Pu system compared with the calculated data from Chiotti et al. [27]: the reference states are liquid Pb and liquid Pu.

4.2. The Pb–Pu system

The calculated phase diagram of the Pb–Pu system compared with all the experimental data [18] used in the present optimization is shown in Figs. 6 and 7. The calculated peritectic reaction, $L + Pb_4Pu_5 \leftrightarrow Pb_3Pu_5$ is in agreement with the temperature reported in the work of Wood et al. [18] although their composition of the liquid phase is smaller than that evaluated in the present work. The temperature of transformation between the αPb_2Pu and βPb_2Pu phases agreed with the experimental data [18] very well. In Fig. 7, the phase boundary between Pb_5Pu_4 and liquid phase is slightly different from the result of Foltyn et al. [29], and this suggests further experimental work to validate the present conclusions. Fig. 8 indicates the calculated Gibbs free energies at 727 °C compared with those obtained by Chiotti [27].

The complete set of the thermodynamic parameters describing the Gibbs free energy of each phase is given in Table 4, and all invariant reactions and special points of the phase diagram are summarized in Table 5, where the experimental data [29] are with available.

Table 4
Parameters for each phase of the Pb–Pu system optimized in this work.

Parameters in each phase (J/mol) with temperature T in Kelvin

Liquid phase, format $(Pb, Pu)_1$

$${}^0L^{Liq}_{Pb,\,Pu} = -77,296 + 25.000T$$
$${}^1L^{Liq}_{Pb,\,Pu} = -3563 - 0.503T$$
$${}^2L^{Liq}_{Pb,\,Pu} = 32,516 - 3.866T$$

A2 εPu phase, format $(Pb, Pu)_1(Va)_3$

$${}^0L^{bcc}_{Pb,\,Pu} = 50,000$$

A1 (Pb, δPu) phase, format $(Pb, Pu)_1(Va)_1$

$${}^0L^{fcc}_{Pb,\,Pu} = 0$$

A6 δ′Pu phase, format $(Pb, Pu)_1$

$${}^0L^{\delta'U}_{Pb,\,Pu} = 0$$

$PbPu_3$ phase, format $(Pb)_{0.25}(Pu)_{0.75}$

$${}^0G^{PbPu_3}_{Pb:Pu} = -23,120 + 0.100T + 0.25{}^0G^{fcc}_{Pb} + 0.75{}^0G^{\alpha Pu}_{Pu}$$

Pb_3Pu_5 phase, format $(Pb)_{0.375}(Pu)_{0.625}$

$${}^0G^{Pb_3Pu_5}_{Pb:Pu} = -35,850 + 4.620T + 0.375{}^0G^{fcc}_{Pb} + 0.625{}^0G^{\alpha Pu}_{Pu}$$

Pb_4Pu_5 phase, format $(Pb)_{0.4444}(Pu)_{0.5556}$

$${}^0G^{Pb_4Pu_5}_{Pb:Pu} = -33300.8 + 2.130T + 0.4444{}^0G^{fcc}_{Pb} + 0.5556{}^0G^{\alpha Pu}_{Pu}$$

βPb_2Pu phase, format $(Pb)_{0.6667}(Pu)_{0.3333}$

$${}^0G^{\beta Pb_2Pu}_{Pb:Pu} = -24,855 + 0.310T + 0.6667{}^0G^{fcc}_{Pb} + 0.3333{}^0G^{\alpha Pu}_{Pu}$$

αPb_2Pu phase, format $(Pb)_{0.6667}(Pu)_{0.3333}$

$${}^0G^{\alpha Pb_2Pu}_{Pb:Pu} = -24,960 + 0.386T + 0.6667{}^0G^{fcc}_{Pb} + 0.3333{}^0G^{\alpha Pu}_{Pu}$$

Pb_3Pu phase, format $(Pb)_{0.75}(Pu)_{0.25}$

$${}^0G^{Pb_3Pu}_{Pb:Pu} = -21,600 + 0.230T + 0.75{}^0G^{fcc}_{Pb} + 0.25{}^0G^{\alpha Pu}_{Pu}$$

Pb_5Pu_4 phase, format $(Pb, Pu)_{0.5556}(Pb, Pu)_{0.4444}$

$${}^0G^{Pb_5Pu_4}_{Pb:Pu} = -29,500 + 1.540T + 0.5556{}^0G^{fcc}_{Pb} + 0.4444{}^0G^{\alpha Pu}_{Pu}$$
$${}^0G^{Pb_5Pu_4}_{Pb:Pb} = 30,000 + {}^0G^{fcc}_{Pb}$$
$${}^0G^{Pb_5Pu_4}_{Pu:Pu} = 10,000 + {}^0G^{\alpha Pu}_{Pu}$$
$${}^0G^{Pb_5Pu_4}_{Pu:Pb} = 10,000 + 0.4444{}^0G^{fcc}_{Pb} + 0.5556{}^0G^{\alpha Pu}_{Pu}$$
$${}^0L^{Pb_5Pu_4}_{Pb:Pb,\,Pu} = -28,000 - 6.300T$$
$${}^0L^{Pb_5Pu_4}_{Pu:Pb,\,Pu} = 0$$
$${}^0L^{Pb_5Pu_4}_{Pb,\,Pu:Pb} = 0$$
$${}^0L^{Pb_5Pu_4}_{Pb,\,Pu:Pu} = 0$$

Table 5
A comparison between the calculated invariant reactions and special points in the Pb–Pu system and the experimental results.

Reaction type	Reaction	Pb (at.%)			T (°C)	Reference
Peritectic	$L + Pb_3Pu_5 \leftrightarrow PbPu_3$	~0.5	37.5	25	896	[29]
		0.9	37.5	25	898	This work
Peritectic	$L + Pb_4Pu_5 \leftrightarrow Pb_3Pu_5$	25.5	44.4	37.5	1333	[29]
		35.7	44.4	37.5	1335	This work
Congruent	$L \leftrightarrow Pb_4Pu_5$		44.4		~1385	[29]
			44.4		1385	This work
Peritectic	$L + Pb_4Pu_5 \leftrightarrow Pb_5Pu_4$	57.5	44.4	55.6	1185	[29]
		60.6	44.4	58.2	1189	This work
Peritectic	$L + Pb_5Pu_4 \leftrightarrow \beta Pb_2Pu$	67.2	57.5	66.7	1129	[29]
		67.1	59.4	66.7	1130	This work
Eutectic	$L \leftrightarrow \beta Pb_2Pu + PbPu_3$	68.8	66.7	75	1124	[29]
		70.1	66.7	75	1121	This work
Congruent	$L \leftrightarrow PbPu_3$		75		1138	[29]
			75		1139	This work
Allotropic	$\alpha Pb_2Pu \leftrightarrow \beta Pb_2Pu$		66.7		1106	[29]
			66.7		1108	This work

5. Conclusions

The phase diagrams and thermodynamic properties of the Pb–U and Pb–Pu binary systems were evaluated by combining the thermodynamic models with the available experimental information. A consistent set of optimized thermodynamic parameters has been derived for describing the Gibbs free energy of each solution phase and intermetallic compound in the Pb–U and Pb–Pu binary systems. Good agreement between the calculated results and most of the experimental data is achieved.

Acknowledgements

This work was supported by the National Natural Science Foundation of China (No. 50771087).

References

[1] D.J. Hill, Nat. Mater. 7 (9) (2008) 680.
[2] D. Olander, J. Nucl. Mater. 389 (2009) 1.
[3] X.J. Liu, Z.S. Li, J. Wang, C.P. Wang, J. Nucl. Mater. 380 (1–3) (2008) 99.
[4] C.P. Wang, P. Yu, X.J. Liu, I. Ohnuma, R. Kainuma, K. Ishida, J. Alloys Compd. 457 (1–2) (2008) 150.
[5] J. Wang, X.J. Liu, C.P. Wang, J. Nucl. Mater. 380 (1–3) (2008) 105.
[6] J. Wang, C.P. Wang, X.J. Liu, J. Nucl. Mater. 374 (1–2) (2008) 79.
[7] C.P. Wang, Y.F. Li, X.J. Liu, K. Ishida, J. Alloys Compd. 458 (1–2) (2008) 208.
[8] Z.S. Li, X.J. Liu, C.P. Wang, J. Alloys Compd. 476 (1–2) (2009) 193.
[9] C.P. Wang, W. Fang, Z.S. Li, X.J. Liu, J. Nucl. Mater. 392 (3) (2009) 525.
[10] V. Sobolev, E. Malambu, H. A Abderrahim, J. Nucl. Mater. 385 (2009) 392.
[11] C. Fazio, G. Benamati, C. Martini, G. Palombarini, J. Nucl. Mater. 296 (2001) 243.
[12] T. Mukaiyama, T. Takizuka, M. Mizumoto, Y. Ikeda, T. Ogawa, A. Hasegawa, H. Takada, H. Takano, Prog. Nucl. Energy 38 (2001) 107.
[13] J.O. Andersson, T. Helander, L. Höglund, P.F. Shi, B. Sundman, Calphad 26 (2002) 273.
[14] H.K. Hardy, Acta Metall. 1 (1953) 202; 2 (1954) 348.
[15] A.T. Dinsdale, Calphad 15 (1991) 317.
[16] O. Redlich, A.T. Kister, Ind. Eng. Chem. 40 (1948) 345.
[17] M. Hillert, L.I. Stafansson, Acta. Chem. Scand. 24 (1970) 3618.
[18] D.H. Wood, E.M. Cramer, P.L. Wallace, W.J. Ramsey, J. Nucl. Mater. 32 (1969) 193.
[19] R.J. Teitel, Trans. Am. Inst. Min, Metall. Eng. 194 (1952) 397.
[20] M.W. Chase, Alloy Phase Diagram 4 (1) (1983) 124.
[21] A. Iandelli, R. Ferro, Ann. Chim. (Rome) 42 (1952) 598.
[22] B.R.T. Frost, J.T. Maskrey, J. Inst. Met. 82 (1953–1954) 171.
[23] R.I. Sheldon, E.M. Foltyn, D.E. Peterson, in: M.E. Kassner, D.E. Peterson (Eds.), Phase Diagrams of Binary Actinide Alloys, ASM International, Materials Park, OH, 1995, p. 202.
[24] C.B. Alcock, P. Grieveson, J. Inst. Met. 90 (1961–1962) 304.
[25] V.A. Lebedev, A.M. Poyarkov, I.F. Nichkov, S.P. Raspopin, Atom Energy 31 (1971) 621.
[26] I. Johnson, H.M. Feder, Thermodynamic of Nuclear Materials, in: Pro. Symp., Vienna, 1962, p. 319.
[27] P. Chiotti, V.V. Akhachinskij, I. Ansara, M.H. Rand, The Chemical Thermodynamic of Actinide elements and Compounds. Part 5: The Actinide Binary Alloys, IAEA, Vienna, 1981.
[28] R.F. Nickerson, J. Nucl. Mater. 32 (1969) 208.
[29] E.M. Foltyn, D.E. Peterson, in: M.E. Kassner, D.E. Peterson (Eds.), Phase Diagrams of Binary Actinide Alloys, ASM International, Materials Park, OH, 1995, p. 372.
[30] F.A. Cafasso, H.M. Feder, I. Johnson, J. Phys. Chem. 66 (7) (1964) 1944.